

One-way surface magnetoplasmon cavity and its application for nonreciprocal devices

Kexin Liu,^{1,2} Amir Torki,¹ and Sailing He^{1,2,*}

¹*Department of Electromagnetic Engineering, School of Electrical Engineering,
Royal Institute of Technology KTH, Stockholm S-100 44, Sweden*

²*Centre for Optical and Electromagnetic Research,
Zhejiang Provincial Key Laboratory for Sensing Technologies,
JORCEP (Sino-Swedish Joint Research Center of Photonics), Zhejiang University, Hangzhou 310058, China*

We theoretically analyze surface magnetoplasmon modes in a compact circular cavity made of magneto-optical material under a static magnetic field. Such a cavity provides two different physical mechanisms for the surface wave to circulate in a unidirectional manner around the cavity, which offers more freedom to realize one-way surface wave. We also show the interaction between this one-way cavity and waveguides, through an example of a circulator, which lays the fundamental groundwork for potential nonreciprocal devices.

PACS numbers: 42.25.-p 78.20.Ls 85.70.Sq

Surface plasmons (SPs) at metal-dielectric interfaces enable confining and manipulating electromagnetic waves on a subwavelength scale [1]. A variety of applications based on the concept of SPs have been achieved at different frequency regimes such as focusing of light beyond the diffraction limit [2], ultracompact nano-lasers [3] and nano-antennas [4, 5]. Applying a static magnetic field on SPs breaks the time-reversal symmetry and gives rise to the nonreciprocal propagation of SPs called surface magnetoplasmons (SMPs) [6–8]. The asymptotic frequencies of SMPs in the forward and backward directions are split by the external magnetic field. This provides a one-way regime for SMPs, i.e., the propagation of the surface wave is only allowed in one direction within the frequency range between two asymptotic frequencies [9, 10]. There are also other mechanisms supporting one-way waves [11–16] including topological protected edge states in photonic crystal. Compared with these however, the mechanism based on SMPs seems more attractive due to its simple configuration.

Recent research has shown that SMPs are immune to backscattering from disorder [9, 17], which might be useful for applications involving isolators. Most results are based on SMPs at a planar interface and use only a single frequency range [9, 10, 17–20]. Since the cavity structure is always compact and at the heart of many photonic components (e.g. High-Q surface-plasmon-polariton whispering-gallery microcavity [21]), it is interesting to study the behavior of SMPs in cavity structures and investigate the physical mechanisms for a one-way SMP cavity mode, i.e., when SMPs circulate around the cavity in a unidirectional manner. Integrating such SMP structures with conventional waveguides is also of particular interest for constructing some nonreciprocal devices.

In this letter, we theoretically analyze SMP modes in a compact circular cavity made of magneto-optical (MO) material under a static magnetic field and demonstrate two different physical mechanisms for one-way cav-

ity modes. The first one results from splitting the asymptotic frequencies for clockwise and anti-clockwise cavity modes, which forms the upper one-way frequency range. The other is obtained by different cut-off frequencies for the lowest clockwise and anti-clockwise cavity modes, which forms the lower one-way frequency range. The circulation directions of SMPs in the cavity are opposite in these two different mechanisms. We also study the interaction between such a one-way SMP cavity and conventional waveguides, which is fundamental for designing nonreciprocal devices. A compact circulator is designed and shown by direct numerical simulations as an example.

We firstly analyze the cavity modes for SMPs to get an insight into the possible one-way regimes. The cavity structure is a circle with radius R surrounded by air in a two-dimensional (2D) system as shown in the insert of Fig. 1(a). The circular cavity is made of a semiconductor which is an MO material at THz frequencies. By applying a static magnetic field in the $+z$ direction and assuming the material is lossless, the relative permittivity tensor of the semiconductor takes the following form in cylindrical coordinates (ρ, φ, z) [6]:

$$\varepsilon = \begin{pmatrix} \varepsilon_1 & i\varepsilon_2 & 0 \\ -i\varepsilon_2 & \varepsilon_1 & 0 \\ 0 & 0 & \varepsilon_3 \end{pmatrix} \quad (1)$$

with $\varepsilon_1 = \varepsilon_\infty(1 - \frac{\omega_p^2}{\omega^2 - \omega_c^2})$, $\varepsilon_2 = \varepsilon_\infty \frac{\omega_c \omega_p^2}{\omega(\omega^2 - \omega_c^2)}$, $\varepsilon_3 = \varepsilon_\infty(1 - \frac{\omega_p^2}{\omega^2})$, where ω is the angular frequency, ω_p is the plasma frequency of the semiconductor, $\omega_c = eB/m^*$ is the electron cyclotron frequency (e and m^* are, respectively, the charge and effective mass of the electron, and B is the applied magnetic field), and ε_∞ is the high-frequency permittivity of the semiconductor. We only consider the TM mode (H_z, E_ρ, E_φ) in this cavity, where $E_z = H_\rho = H_\varphi = 0$. Maxwell's equations yield

$$E_\varphi = \frac{1}{i\omega\varepsilon_0(\varepsilon_1^2 - \varepsilon_2^2)} \left(\frac{i\varepsilon_2}{\rho} \frac{\partial}{\partial \varphi} - \varepsilon_1 \frac{\partial}{\partial \rho} \right) H_z \quad (2a)$$

$$E_\rho = \frac{1}{i\omega\epsilon_0(\epsilon_1^2 - \epsilon_2^2)} \left(\frac{\epsilon_1}{\rho} \frac{\partial}{\partial \varphi} + i\epsilon_2 \frac{\partial}{\partial \rho} \right) H_z \quad (2b)$$

$$\frac{1}{\rho} \frac{\partial}{\partial \rho} \rho E_\varphi - \frac{1}{\rho} \frac{\partial}{\partial \varphi} E_\rho = -i\omega\mu_0 H_z \quad (2c)$$

Taking the field $H_z = \psi(\rho)e^{im\varphi}$, where m is an integer indicating the azimuthal mode number, we obtain the following differential equation from Eq. (2):

$$\left[\frac{\partial}{\partial \rho^2} + \frac{1}{\rho} \frac{\partial}{\partial \rho} + (k^2 - \frac{m^2}{\rho^2}) \right] \psi(\rho) = 0 \quad (3)$$

where $k^2 = \omega^2\mu_0\epsilon_0\epsilon_v$, with Voigt permittivity $\epsilon_v = \epsilon_1 - \epsilon_2^2/\epsilon_1$. Inside the circle ($\rho \leq R$), the solution for Eq. (3) is the Bessel function of the first kind $J_m(k\rho)$. Outside the circle ($\rho > R$), for outgoing waves, the solution for Eq. (3) is the Hankel function of the first kind $H_m^{(1)}(k_0\rho)$, where k_0 is the wave vector in air. Therefore, the solution is given by

$$\psi(\rho) = \begin{cases} A \cdot J_m(k\rho) & \rho \leq R \\ C \cdot H_m^{(1)}(k_0\rho) & \rho > R \end{cases} \quad (4)$$

According to the boundary conditions that H_z and E_φ are continuous at $\rho = R$, we obtain the following eigenfrequency equation of the cavity modes:

$$\frac{J_m(kR)}{H_m^{(1)}(k_0R)} = \frac{(\epsilon_2 m/R) \cdot J_m(kR) + \epsilon_1 k \cdot J_m'(kR)}{(\epsilon_1^2 - \epsilon_2^2)k_0 \cdot H_m^{(1)'}(k_0R)} \quad (5)$$

We can solve Eq. (5) numerically for each given azimuthal mode number m and obtain the dispersion relation between the eigenfrequency and the mode number m . The linear term $(\epsilon_2 m/R) \cdot J_m(kR)$ with respect to m , which originates from the off-diagonal element of the permittivity tensor, breaks the left-right symmetry of the dispersion relation. Therefore, the solutions for Eq. (5) and also the field distributions are different for the cavity modes $|+m\rangle$ and $|-m\rangle$, where $|+m\rangle$ and $|-m\rangle$ represent the modes with positive and negative mode numbers, respectively. In addition, we only investigate the fundamental radial mode, since it is the most confined of the radial modes.

We take a semiconductor disk made of InSb with $R = 250 \mu\text{m}$ as an example to show the solution for Eq. (5). At room temperature, the semiconductor InSb takes the following parameters: $\epsilon_\infty = 15.6$, $f_p = \omega_p/2\pi = 2 \text{ THz}$ and $m^* = 0.014m_0$ (m_0 is the free electron mass) [22]. We study three cases with increasing applied magnetic field $B = 0 \text{ T}$ ($\omega_c = 0$), $B = 0.025 \text{ T}$ ($\omega_c = \omega_p/40$) and $B = 0.1 \text{ T}$ ($\omega_c = \omega_p/10$) along the $+z$ axis and solve Eq. (5) numerically. The solutions for those three cases are illustrated in Fig. 1(a), where the dots show the dispersion relations and the gray region represents the region above the air light line. The air light line is determined by

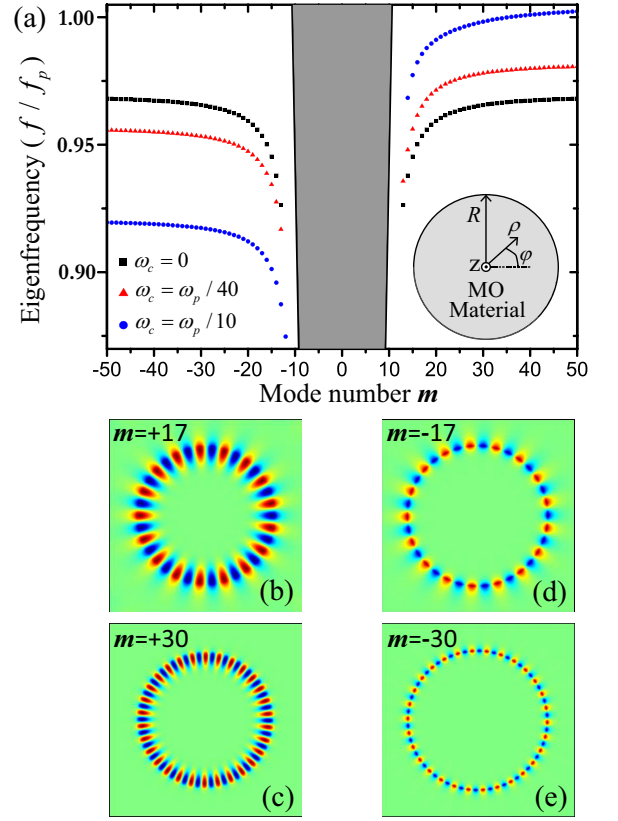


FIG. 1: (a) The dispersion relation between the eigenfrequency and azimuthal mode number m of the circular cavity. The circular cavity with radius R is surrounded by air in the two-dimensional (2D) system as shown in the insert. The cavity is made of the semiconductor InSb, which is a magnetooptical (MO) material at THz frequencies. Three cases with increasing electron cyclotron frequency $\omega_c = 0$ (black square dots), $\omega_c = \omega_p/40$ (red triangular dots) and $\omega_c = \omega_p/10$ (blue circular dots) are plotted. The gray region represents the region above the light line. The distributions of the modal field H_z are shown in (b) $m = +17$, (c) $m = +30$, (d) $m = -17$ and (e) $m = -30$, respectively, when $\omega_c = \omega_p/10$.

$f = mc/2\pi R$. The dispersion relations start from different cutoff frequencies and approach different asymptotic frequencies in these three cases. Firstly, in the absence of an external magnetic field ($B = 0 \text{ T}$, $\omega_c = 0$, black square dots), the dispersion relation is symmetric, as the time-reversal symmetry is preserved. When $m \rightarrow \pm\infty$, the mode has an infinite azimuthal wave vector, and the asymptotic frequency is $f_s = (\omega_p/2\pi)\sqrt{\epsilon_\infty/(\epsilon_\infty + \epsilon_{\text{air}})}$, which is the same result for SPs without magnetization. When m is very small, due to the limitation of the air light line, the corresponding eigenfrequency can be a complex number, which corresponds to a radiative mode [23]. The lowest mode with a real eigenfrequency gives the cutoff frequency for nonradiative modes. In this letter, we only consider the nonradiative modes. Note that when $R \rightarrow \infty$, the cutoff frequency will approach zero, which is exactly the case for SPs at a planar interface.

The curvature of the interface enables one to achieve the cutoff frequency above zero. For the second case with $B = 0.025\text{ T}$ ($\omega_c = \omega_p/40$, red triangular dots), the dispersion relation is asymmetric, and the asymptotic frequencies are split by the external magnetic field. The $+m$ branch of the dispersion relation is higher than the dispersion relation with $B = 0\text{ T}$, while the $-m$ branch is lower than the one with $B = 0\text{ T}$. When $m \rightarrow \pm\infty$, applying the formulas $J_{m \rightarrow +\infty}(s) \sim (1/\sqrt{2\pi m}) \cdot (es/2m)^m$, $H_{m \rightarrow +\infty}^{(1)}(s) \sim (-i\sqrt{2}/\sqrt{\pi m}) \cdot (es/2m)^{-m}$, $J_{-m}(s) = (-1)^m J_m(s)$ and $H_{-m}(s) = (-1)^m H_m(s)$ in Eq. (5), we obtain the following asymptotic frequencies

$$f_{\pm\infty} = \frac{1}{4\pi} \left(\sqrt{\omega_c^2 + 4\omega_p^2 \frac{\varepsilon_\infty}{\varepsilon_\infty + \varepsilon_{air}}} \pm \omega_c \right) \quad (6)$$

which are the same as SMPs at a planar interface discussed in [17]. Within the one-way frequency range $f_{-\infty} < f < f_{+\infty}$, there only exists $|+m\rangle$ modes, and SMPs can only circulate around the cavity anti-clockwise. Furthermore, there does exist different cutoff frequencies for $|+m\rangle$ and $|-m\rangle$ cavity modes. The cutoff frequency f_{+c} of the $|+m\rangle$ mode is higher than the cutoff frequency f_{-c} of the $|-m\rangle$ mode, so there is another one-way frequency range. Within $f_{-c} < f < f_{+c}$, there only exists $|-m\rangle$ modes, and SMPs can only circulate around the cavity clockwise. In the third case, we apply a stronger magnetic field $B = 0.1\text{ T}$ ($\omega_c = \omega_p/10$, blue circular dots). The applied strong magnetic field considerably breaks the symmetry of the dispersion relation. The cutoff frequency f_{+c} of the $|+m\rangle$ mode can be lifted higher than the asymptotic frequency $f_{-\infty}$ of the $|-m\rangle$ mode. In this case, the modes $|+m\rangle$ and $|-m\rangle$ are separated in completely different frequency ranges. The $|+m\rangle$ modes are within $f_{+c} < f < f_{+\infty}$ and SMPs can only circulate anti-clockwise in this frequency range. The $|-m\rangle$ modes are within $f_{-c} < f < f_{-\infty}$ and SMPs can only circulate clockwise in this frequency range. The circulation directions are opposite in these two different one-way frequency ranges. This interesting feature offers more freedom, both in the one-way direction and in the frequency range, for designing nonreciprocal components.

To verify the theoretical results obtained from Eq. (5), we also solve the eigenfrequency of the cavity mode and calculate the modal field distributions by a finite element method (FEM) in the commercial software COMSOL. The deviation of the FEM results from the results obtained by Eq. (5) is less than 1%. The modal field (H_z) distributions of the cavity modes $|\pm 17\rangle$ and $|\pm 30\rangle$ for $B = 0.1\text{ T}$ are plotted in Fig. 1(b)-1(d), respectively. The field is confined at the boundary of the cavity and this confinement increases with $|m|$. We also note that the field distributions are different for the $|+m\rangle$ and $|-m\rangle$ modes, since the strong external magnetic field breaks the symmetry. To clearly demonstrate the circulation direction of SMPs, we made videos of the harmonic wave

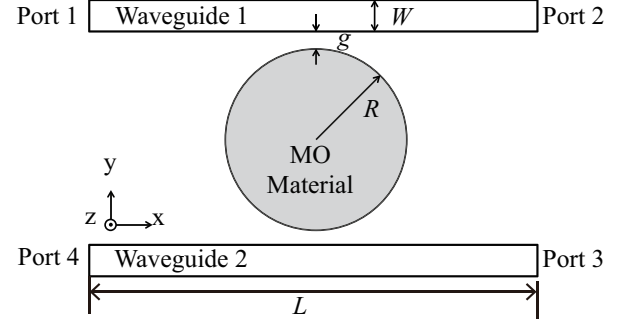


FIG. 2: The schematic of the circulator. The circulator consists of a circular cavity with $R = 250\text{ }\mu\text{m}$ and two straight dielectric waveguides. The straight waveguides are symmetric about the center of the cavity. The width of the straight waveguides is $W = 40\text{ }\mu\text{m}$, the length is $L = 8R$ and the dielectric constant of the waveguides is $\varepsilon_d = 5$. In addition, the gap between the cavity and the waveguide is $g = 20\text{ }\mu\text{m}$.

propagation around the cavity at the eigenfrequencies of modes $|\pm 17\rangle$. To excite these modes, a magnetic current point source is placed at the boundary of the cavity. The field H_z of the wave is recorded (see supplementary material online).

In this section, we study the interaction between the one-way SMP cavity and the conventional waveguides, which is fundamental for designing nonreciprocal devices. We use the one-way SMP cavity to construct a circulator as an example. The circulator consists of a circular cavity and two straight dielectric waveguides as shown in Fig. 2. The parameters of the cavity are the same as those in the third case discussed above. The straight waveguides are symmetric about the center of the cavity. We denote the width, length and relative permittivity of the waveguides by W , L and ε_d . The gap between the cavity and the waveguide is g . The dispersion relation for the fundamental guiding TM mode (H_z, E_x, E_y) in the waveguide can be obtained by solving

$$k_2 = \frac{k_1}{\varepsilon_d} \tan\left(\frac{k_1 W}{2}\right) \quad (7)$$

where $k_1 = \sqrt{\omega^2 \mu_0 \varepsilon_0 \varepsilon_d - \beta^2}$, $k_2 = \sqrt{\beta^2 - \omega^2 \mu_0 \varepsilon_0}$ and β is the propagation constant [24]. To achieve a strong interaction between the guiding modes and the cavity mode, the phase matching condition [25] is required:

$$\beta(f_m) \cong \beta_e(m) \left(1 - \frac{g}{2R}\right) \quad (8)$$

where f_m is the eigenfrequency of the cavity mode $|m\rangle$, and $\beta_e(m)$ is the equivalent propagation constant of the cavity mode $|m\rangle$. When the modal field is confined well at the boundary of the cavity, $\beta_e = m/R$. The term $(1 - g/2R)$ includes the effect of the curvature at the cavity boundary on the propagation constant as seen by the

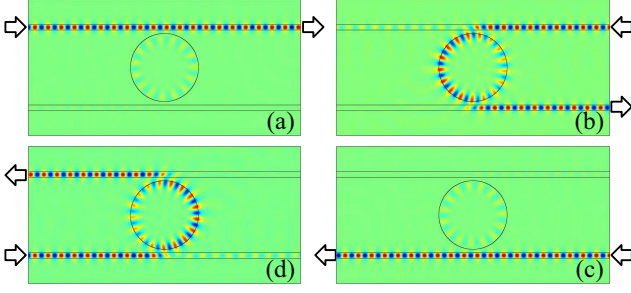


FIG. 3: Simulation result of wave propagation at the resonance frequency for $m = +17$. In (a)-(d), input power is at Port 1, 2, 3 and 4, respectively.

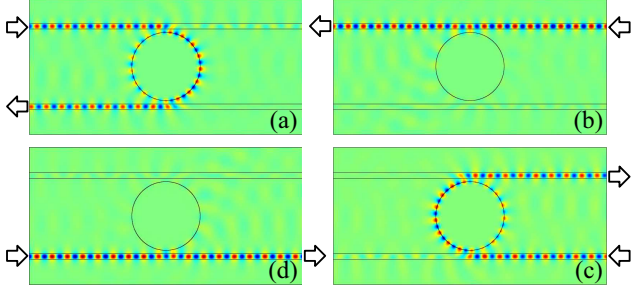


FIG. 4: Simulation result of wave propagation at the resonance frequency for $m = -17$. In (a)-(d), input power is at Port 1, 2, 3 and 4, respectively.

straight waveguide approximately [24]. Due to the asymmetric dispersion relation of the cavity mode, coupling occurs in a uni-directional manner between the guiding mode and the cavity mode within the one-way frequency ranges. We set $m = 17$ and find that the structure with $W = 40 \mu\text{m}$, $\varepsilon_d = 5$ and $g = 20 \mu\text{m}$ satisfies Eq. (8). In addition, the length is $L = 8R = 2000 \mu\text{m}$ and Ports 1-4 are labeled at the end of the waveguides.

Next, we study the performance of the circulator at both one-way frequency ranges. As the radius of the cavity is in the order of wavelength, and the structure of the circulator is compact, we use the FEM method to simulate the performance of the circulator. For the upper one-way frequency range, in which only $|+m\rangle$ exists, Fig. 3(a)-3(d) show the wave propagation at the resonance frequency for $m = +17$, when the input power is at Port 1, 2, 3 and 4, respectively. The input wave from Port 1 is not coupled with the cavity mode and goes out at Port 2 [Fig. 3(a)], while the input wave from Port 2 is coupled with the cavity mode and goes out at Port 3 [Fig. 3(b)]. The wave travels in the order Port1→Port2→Port3→Port4→Port1. For the lower one-way frequency range, in which only $|-m\rangle$ exists, Fig. 4(a)-4(d) show the wave propagation at the resonance frequency for $m = -17$, when the input power is at Port 1, 2, 3 and 4, respectively. The wave travels in the order Port1→Port4→Port3→Port2→Port1.

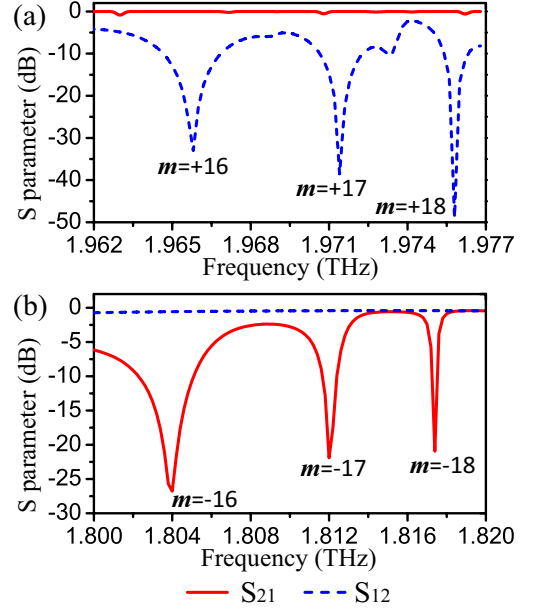


FIG. 5: Calculated S parameters for the circulator. (a) S parameters within the upper one-way frequency range. The dips are the resonance frequencies corresponding to $m = +16, +17, +18$. (b) S parameters within the lower one-way frequency range. The dips are the resonance frequencies corresponding to $m = -16, -17, -18$.

The properties of transmission and isolation are shown by the calculated S parameters in Fig. 5. Within the upper one-way frequency range [Fig. 5(a)], the transmission coefficient S_{21} (red solid line) from Port 1 to Port 2 is close to 0 dB, which indicates that the guided wave from Port 1 is not coupled with SMPs in the cavity. The small losses (small dips of S_{21}) are caused by a weak coupling with some other whispering-gallery-like modes inside the cavity. This coupling can be eliminated by increasing the gap between the cavity and the waveguides (not shown here). The three dips of the isolation S_{12} (blue dashed line) are the resonance frequencies corresponding to $m = +16, +17, +18$. The resonance frequencies are very close to the eigenfrequencies of the cavity modes $|+16\rangle$, $|+17\rangle$, $|+18\rangle$, as the cavity modes are perturbed slightly by the 2 straight waveguides. Within the lower one-way frequency range [Fig. 5(b)], the transmission coefficient S_{12} (blue dashed line) from Port 2 to Port 1 is close to 0 dB. The three dips of the isolation S_{21} (red solid line) are the resonance frequencies corresponding to $m = -16, -17, -18$. The resonance frequencies are shifted a little from their corresponding eigenfrequencies of $|-16\rangle$, $|-17\rangle$ and $|-18\rangle$, since the geometric structure is designed to fulfill the phase matching condition Eq. (8) at $m = +17$. All the dips are lower than -20 dB, indicating good isolation performance.

In conclusion, we have theoretically analyzed the SMP mode in a compact circular MO cavity under a mag-

netic field. In such a cavity, we have found that the different asymptotic and different cut-off frequencies for clockwise and anti-clockwise modes lead to two one-way frequency ranges for SMPs in the cavity. These multiple mechanisms for achieving one-way SMPs offer more freedom, both in the one-way direction and in the frequency range, for designing nonreciprocal photonic components. We also have studied the application of this cavity in a four-port circulator as an example to show the interaction between the one-way SMP cavity and waveguides, which is the heart of nonreciprocal devices. We believe that the mechanisms we found in the cavity will provide people more ways to manipulate SPs and our idea may be useful in a variety of potential applications ranging from THz signal isolation to isolators on chips.

This work is supported by Swedish VR grant (No. 621-2011-4620) and AOARD. The partial support of the National Natural Science Foundation of China (Nos. 61178062 and 91233208) is also acknowledged. Kexin Liu thanks the China Scholarship Council (CSC) No. 201406320056. Amir Torki thanks the Swedish Institute Scholarship (SI).

* corresponding author: sailing@kth.se

- [1] S. A. Maier, *Plasmonics: Fundamentals and Applications* (Springer-Verlag, Berlin, 2007).
- [2] W. L. Barnes, A. Dereux, and T. W. Ebbesen, *Nature* **424**, 824 (2003).
- [3] L. Novotny and N. F. van Hulst, *Nature Photonics* **5**, 83 (2011).
- [4] M. A. Noginov et al., *Nature* **460**, 1110 (2009).
- [5] D. Dregely et al., *Nature Communications* **2**, 267 (2011).
- [6] J. J. Brion, R. F. Wallis, A. Hartstein, and E. Burstein, *Physical Review Letters* **28**, 1455 (1972).
- [7] M. S. Kushwaha and P. Halevi, *Physical Review B* **36**, 5960 (1987).
- [8] M. S. Kushwaha and B. D. Rouhani, *Physical Review B* **43**, 9021 (1991).
- [9] Z. Yu, G. Veronis, Z. Wang, and S. Fan, *Physical Review Letters* **100**, 023902 (2008).
- [10] B. Hu, Q. J. Wang, and Y. Zhang, *Optics Letters* **37**, 1895 (2012).
- [11] F. D. M. Haldane and S. Raghu, *Physical Review Letters* **100**, 013904 (2008).
- [12] Z. Wang, Y. D. Chong, J. D. Joannopoulos, and M. Soljacic, *Physical Review Letters* **100**, 013905 (2008).
- [13] Z. Wang, Y. Chong, J. D. Joannopoulos, and M. Soljacic, *Nature* **461**, 772 (2009).
- [14] A. B. Khanikaev, A. V. Baryshev, M. Inoue, and Y. S. Kivshar, *Applied Physics Letters* **95**, 011101 (2009).
- [15] M. C. Rechtsman et al., *Nature* **496**, 196 (2013).
- [16] A. B. Khanikaev, et al., *Nature Materials* **12**, 233 (2013).
- [17] L. Shen and Y. You and Z. Wang and X. Deng, *Opt. Express* **23**, 950 (2015).
- [18] X. Zhang, W. Li, and X. Jiang, *Applied Physics Letters* **100**, 041108 (2012).
- [19] V. Kuzmiak, S. Eyderman, and M. Vanwolleghem, *Physical Review B* **86**, 045403 (2012).
- [20] F. Abbasi, A. R. Davoyan, and N. Engheta, *New Journal of Physics* **17**, 063014 (2015).
- [21] B. Min et al., *Nature* **457**, 455 (2009).
- [22] J. G. Rivas, C. Janke, P. H. Bolivar, and H. Kurz, *Opt. Express* **13**, 847 (2005).
- [23] C. A. Pfeiffer, E. N. Economou, and K. L. Ngai, *Physical Review B* **10**, 3038 (1974).
- [24] K. Okamoto, *Fundamentals of Optical Waveguides* (Academic, San Diego, 2006).
- [25] D. R. Rowland and J. D. Love, *IEE Proc. J.* **140**, 177 (1993).